

# Contribution to the Calorimetric Study of the Bi-Ni-Sn Ternary System: Experimental and Theoretical Data

Imane Brogi<sup>1</sup>, Meryem Rechchach<sup>1</sup>, Mouloud El Moudane<sup>2</sup>, Abdelaziz Sabbar<sup>1,\*</sup>

<sup>1</sup> Laboratory of Spectroscopy, Molecular Modeling, Materials, Nanomaterials, Water and Environment, CERNE2D, Mohammed V University in Rabat, Faculty of Sciences, Av. Ibn Battouta, B.P. 1014 Rabat, Morocco

<sup>2</sup> Laboratory of Materials, Nanotechnology and Environment, Faculty of Sciences, Mohammed V University in Rabat, Av. Ibn Battouta, P. O. Box 1014 Agdal-Rabat, Morocco

\* Correspondence: [asabbar2001@yahoo.fr](mailto:asabbar2001@yahoo.fr) (A.S.);

Scopus Author ID 6506508792

Received: date; Accepted: date; Published: date

**Abstract:** In the present work, the partial and integral enthalpies of mixing ternary Bi-Ni-Sn liquid alloys were measured at 1000°C using the drop calorimetry method. The measurements were performed along five binary isopleths  $\text{Bi}_x\text{Sn}_{1-x}$  by addition of nickel and three binary isopleths  $\text{Bi}_x\text{Ni}_{1-x}$  by addition of tin. These same thermodynamic quantities were also calculated using three geometric models. A zone of non-miscibility was identified. The study showed that the integral and partial enthalpies are exothermic, particularly for nickel-rich sections (F, G, and H sections). On the other hand, this work has indicated the possible presence of a domain of immiscibility as reported in other works.

**Keywords:** Integral and partial thermodynamic quantities; calorimetry technique; Bi-Ni-Sn system; geometrical models.

© 2022 by the authors. This article is an open-access article distributed under the terms and conditions of the Creative Commons Attribution (CC BY) license (<https://creativecommons.org/licenses/by/4.0/>).

## 1. Introduction

Due to its good physical, chemical, and mechanical properties and low cost, traditional Sn-Pb solder (eutectic or near eutectic) have been widely used in the electronics industry to assemble electronic components. However, the use of lead has become very limited due to its toxic nature and therefore, its harmful effects on the environment and health. Since the introduction of the European directive [1] requiring the limitation of the use of lead, several binary, ternary, and quaternary alloys... have been developed and studied as lead-free solders. In this regard, substantial research was recently conducted to develop new lead-free solders [2-16].

Sn-Bi and Sn-Ni-containing solders may be promising candidates. On the other hand, Bi and Ni can be used as additional components and/or contact materials (substrate). Information on thermodynamic properties such as enthalpy of mixing in the Bi-Ni-Sn system is considered an indispensable contribution to the systematic design of lead-free solders. To the authors' best knowledge, only one experimental result of enthalpies of formation of Bi-Ni-Sn liquid alloys has already been reported [17]. The measurements of Vassilev *et al.* [17] have been realized for the ternary liquid phase at different temperatures using direct drop calorimetry.

This paper studies experimental enthalpies of mixing in the liquid Bi-Ni-Sn alloys in a large compositional range at 1000°C. Measurements have been done along eight sections

$x_{\text{Bi}}/x_{\text{Sn}} = 0.34/0.66$ ;  $0.50/0.50$ ;  $0.65/0.35$ ;  $0.74/0.26$ ;  $0.89/0.11$  by adding nickel, and  $x_{\text{Bi}}/x_{\text{Ni}} = 0.70/0.30$ ;  $0.76/0.24$ ;  $0.80/0.20$  by adding tin. The objective of this study is to have an idea of the interaction between a Bi-Sn solder and a nickel as a substrate. On the other hand, this work is carried out to verify the existence of a possible domain of non-miscibility (liquid-liquid). Additionally, the enthalpies of mixing were estimated using Kohler [18] as a symmetric model, Toop [19] as an asymmetric model, and Chou [20] as a general solution model. The estimated and measured values are compared to each other.

## 2. Literature data

Predel and Ruge [21] determined the enthalpy of formation of intermetallic compound BiNi by calorimetric technique. The heat capacities of BiNi in the temperature range of 37-577°C were measured by Perring *et al.* [22] using differential scanning calorimetry. Vassilev *et al.* [23] have published thermodynamic assessments and reported this intermetallic compound's enthalpy of formation using the CALPHAD method. Samui *et al.* [24] have determined the enthalpy of decomposition of Bi<sub>3</sub>Ni and BiNi intermetallic compounds. Recently, the enthalpy of mixing of liquid phase at different temperatures was measured at low compositions of Ni ( $x_{\text{Ni}} \leq 0,2$ ) [25]. More recently, El Maniani *et al.* [26] and Fima and Flandofer [27] have measured this thermochemical function in the binary Bi-Ni liquid alloys. The results of both calorimetric measurements are nearly similar at 1000°C.

Hultgren *et al.* [28] reported a review of all thermodynamic values available for Bi-Sn from investigations performed until 1965. The investigation of thermodynamic properties by calorimetric measurements are determined by Yazawa *et al.* [29] and Sharkey and Pool [30], while the emf method was carried out by Seltz and Dunkerley [31]. The results of the different measurements show a large scatter and some contradictions. In 1990, Cho *et al.* [32] reinvestigated this system using the same method. More recent experimental results by emf measurements given by Asryan and Mikula [33] have shown that the enthalpy of mixing versus composition was asymmetric.

Calorimetric methods have investigated the thermodynamic parameters in the Ni-Sn system several times. The results published until 1971 were compiled by Hultgren *et al.* [28]. The enthalpy in the liquid Ni-Sn alloys was investigated experimentally [34-36]. According to Luck *et al.* [35], the enthalpy of mixing depends on temperature between 1387 and 1502°C, while such independence has been reported in the temperature range 594-1306°C by Haddad *et al.* [36]. According to Luck *et al.* [35], the enthalpy of mixing depends on temperature between 1387 and 1502°C, while Haddad *et al.* [36] reported independence between 594 and 1306°C. The same behavior was observed by Flandorfer *et al.* [37] during the experimental study at three temperatures (1173, 1250, and 1500 °C) using the drop calorimetric technique. This thermodynamic quantity was calculated at 1307 °C by Glibin *et al.* [38] using a modified quasi-chemical model. Several thermodynamic assessments have been reported [39-41].

Concerning Bi-Ni-Sn ternary system, the enthalpies of the formation of three liquid alloys were measured by Vassilev *et al.* [17] at 560, 600, and 660 °C using direct drop calorimetry.

## 3. Experiments

The calorimetric measurements and the equations for calculating the partial and integral enthalpies were made according to the same method used in our previous work [26]. The

enthalpies of mixing were determined at 1000°C along eight isopleths (Figure 1) with  $\text{Bi}_x\text{Sn}_{1-x} + \text{Ni}$  (A, B, C, D, and E sections) and  $\text{Bi}_x\text{Ni}_{1-x} + \text{Sn}$  (F, G, and H sections).

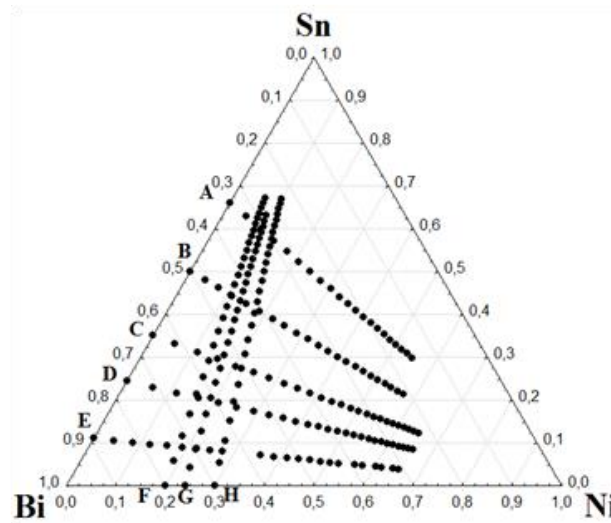


**Figure 1.** Measured sections (A-H) in the ternary Bi-Ni-Sn system at 1000°C.

#### 4. Theoretical Study

Three different extrapolations models such as Kohler [18], Toop [19], and Chou [20] have been used, and the predicted enthalpy values were compared with the measured ones.

The equations representing the three models used are given below where  $\Delta_{\text{mix}}H_{123}$ ,  $x_1$ ,  $x_2$  and  $x_3$  are the integral enthalpy and the mole fractions of a ternary 1-2-3 alloys.

Kholer's model [18]:

$$\Delta_{\text{mix}}H_{123} = (x_1 + x_2)^2 \Delta_{\text{mix}}H_{12} \left( \frac{x_1}{x_1 + x_2}; \frac{x_2}{x_1 + x_2} \right) + (x_1 + x_3)^2 \Delta_{\text{mix}}H_{13} \left( \frac{x_1}{x_1 + x_3}; \frac{x_3}{x_1 + x_3} \right) + (x_2 + x_3)^2 \Delta_{\text{mix}}H_{23} \left( \frac{x_2}{x_2 + x_3}; \frac{x_3}{x_2 + x_3} \right)$$

Toop's model [19]:

$$\Delta_{\text{mix}}H_{123} = (x_2 + x_3)^2 \Delta_{\text{mix}}H_{23} \left( \frac{x_2}{x_2 + x_3}; \frac{x_3}{x_2 + x_3} \right) + \frac{x_2}{(1 - x_1)} \Delta_{\text{mix}}H_{12}(x_1; 1 - x_1) + \frac{x_3}{(1 - x_1)} \Delta_{\text{mix}}H_{13}(x_1; 1 - x_1)$$

Chou's model [20]:

$$\Delta_{\text{mix}}H_{123} = x_1 x_2 \sum_v L_{12}^{(v)} (x_1 - x_2)^v + x_2 x_3 \sum_v L_{23}^{(v)} (x_2 - x_3)^v + x_3 x_1 \sum_v L_{31}^{(v)} (x_3 - x_1)^v + x_1 x_2 x_3 f$$

where,

$$f = (2\xi_{12} - 1)[L_{12}^2((2\xi_{12} - 1)x_3 + 2(x_1 - x_2)) + L_{12}^1] + (2\xi_{23} - 1)[L_{23}^2((2\xi_{23} - 1)x_1 + 2(x_2 - x_3)) + L_{23}^1] + (2\xi_{31} - 1)[L_{31}^2((2\xi_{31} - 1)x_2 + 2(x_3 - x_1)) + L_{31}^1]$$

$L_{ij}^{(v)}$  are the interaction parameters of binary "ij".  $\xi_{ij}$  is the similarity coefficients for three binaries defined by the deviation sum of squares  $\eta_i$ :

$$\xi_{12} = \frac{\eta_I}{\eta_I + \eta_{II}} \xi_{23} = \frac{\eta_{II}}{\eta_{II} + \eta_{III}} \xi_{31} = \frac{\eta_{III}}{\eta_{III} + \eta_I}$$

$$\eta_I = \int_0^1 (\Delta_{\text{mix}}H_{12} - \Delta_{\text{mix}}H_{13})^2 dX_1 \eta_{II} = \int_0^1 (\Delta_{\text{mix}}H_{21} - \Delta_{\text{mix}}H_{23})^2 dX_2$$

$$\eta_{III} = \int_0^1 (\Delta_{\text{mix}}H_{31} - \Delta_{\text{mix}}H_{32})^2 dX_3$$

and

$$X_{1(12)} = x_1 + x_3 \xi_{12} X_{2(23)} = x_2 + x_1 \xi_{23} X_{3(31)} = x_3 + x_2 \xi_{31}$$

$\Delta_{\text{mix}}H_{ij}$  is the enthalpy of mixing in binary ij system expressed as:

$$\Delta_{\text{mix}}H_{ij} = X_i X_j \sum_v L_{ij}^{(v)} (X_i - X_j)^v$$

$X_i$  and  $X_j$  are the mole fraction of component "i" and "j" in "ij" binary system.

## 5. Results and Discussion

### 5.1. Experimental results.

Measurements have been done along eight starting binary sections A-H (Table 2) by adding nickel to  $x_{\text{Bi}}/x_{\text{Sn}} = 0.34/0.66; 0.50/0.50; 0.65/0.35; 0.74/0.26; 0.89/0.11$ , and by adding tin  $x_{\text{Bi}}/x_{\text{Ni}} = 0.70/0.30; 0.76/0.24; 0.80/0.20$ .

**Table 1.** Starting binary sections.

A	B	C	D	E	F	G	H
Bi <sub>0.34</sub> Sn <sub>0.66</sub>	Bi <sub>0.50</sub> Sn <sub>0.50</sub>	Bi <sub>0.65</sub> Sn <sub>0.35</sub>	Bi <sub>0.74</sub> Sn <sub>0.26</sub>	Bi <sub>0.89</sub> Sn <sub>0.11</sub>	Bi <sub>0.80</sub> Ni <sub>0.20</sub>	Bi <sub>0.76</sub> Ni <sub>0.24</sub>	Bi <sub>0.70</sub> Ni <sub>0.30</sub>

All experimental calorimetric results of the investigated Bi-Ni-Sn system are collected in Table 2, which contains the experimental information such as starting amounts (Bi<sub>x</sub>Sn<sub>1-x</sub> and Bi<sub>x</sub>Ni<sub>1-x</sub>), added amounts of Sn or Ni (drop metal), corresponding heat effects (Q), experimental  $\Delta_{\text{mix}}H$  of the liquid alloys, and partial quantity of mixing ( $\Delta\bar{H}_M$ ) of the added metal M (M= Ni or Sn).

The enthalpy values of the starting binary Bi<sub>x</sub>Sn<sub>1-x</sub> and Bi<sub>x</sub>Ni<sub>1-x</sub> alloys are taken from the works of Asryan and Mikula [33] and El Maniani *et al.* [26], respectively.

Figure 2 shows the curves  $\Delta_{\text{mix}}H$  versus Ni-compositions for all investigated isopleths. As it can be seen, a decrease in the enthalpy of mixing is observed as the amount of Ni increases. The mixing enthalpy curves show a kink for all sections except in section A. The coordinates of this kink ( $x_{\text{Ni(kink)}}, \Delta_{\text{mix}}H_{\text{(kink)}}$ ) depend on the studied section. As the amount of Bi increases, the composition of Ni ( $x_{\text{Ni(kink)}}$ ) decreases and the corresponding enthalpy of mixing ( $\Delta_{\text{mix}}H_{\text{kink}}$ ) increases (Table 3).

**Table 2.** Partial and integral enthalpies of mixing in the liquid Bi-Ni-Sn alloys; initial state  $\Delta_{\text{mix}}H$ : pure liquid metals at 1000°C.

Mole dropped $n_{\text{Ni}}$ (mmol)	Heateffect $Q(\text{J})$	Partial enthalpy		Integralenthalpy	
		$x_{\text{Ni}}^*$	$\Delta\bar{H}_{\text{Ni}}(\text{J.mol}^{-1})$	$x_{\text{Ni}}$	$\Delta_{\text{mix}}H(\text{J.mol}^{-1})$
<b>Section A; starting amount : n(Bi) = 3.1574mmol ; n(Sn) = 6.0912mmol</b>					
				0	94.07
0.4723	4639	0.0243	-35711	0.0486	-1645
0.4740	4766	0.0707	-35479	0.0928	-3218

Mole dropped $n_{Ni}$ (mmol)	Heateffect $Q(J)$	Partial enthalpy		Integralenthalpy	
		$x_{Ni}^*$	$\overline{\Delta H_{Ni}}(J.mol^{-1})$	$x_{Ni}$	$\Delta_{mix}H(J.mol^{-1})$
0.4788	4772	0.1132	-35568	0.1335	-4670
0.4998	2763	0.1529	-40007	0.1723	-6250
0.5204	9195	0.1907	-27865	0.2091	-7212
0.5283	9321	0.2262	-27891	0.2433	-8106
0.5312	10490	0.2590	-25790	0.2748	-8843
0.5384	8884	0.2895	-29035	0.3042	-9661
0.5486	6134	0.3180	-34355	0.3318	-10639
0.5519	11566	0.3446	-24581	0.3574	-11174
0.5578	7588	0.3694	-31932	0.3814	-11949
0.5661	7376	0.3927	-32504	0.4039	-12698
0.5681	12615	0.4145	-23329	0.4250	-13074
0.5770	7989	0.4349	-31689	0.4449	-13719
0.6168	9200	0.4548	-30620	0.4647	-14322
0.6279	11102	0.4741	-27853	0.4835	-14796
0.6300	7294	0.4923	-33957	0.5010	-15448
0.6337	14349	0.5093	-22891	0.5175	-15694
0.6616	6188	0.5256	-36183	0.5336	-16377
<b>Section B; starting amount : n(Bi) = 4.2434mmol ; n(Sn) = 4.3384mmol</b>					
				0	105
0.3554	5374	0.0199	-32252	0.0398	-1182
0.3563	5365	0.0582	-32320	0.0766	-2376
0.3919	6191	0.0953	-31576	0.1139	-3557
0.4260	7390	0.1326	-30028	0.1513	-4673
0.4352	7467	0.1688	-30215	0.1863	-5727
0.4808	5683	0.2040	-35555	0.2218	-7027
0.4869	6818	0.2382	-33371	0.2547	-8141
0.5310	8235	0.2711	-31864	0.2875	-9187
0.5358	7189	0.3027	-33955	0.3179	-10242
0.5420	5372	0.3320	-37462	0.3460	-11366
0.5527	2952	0.3593	-42033	0.3725	-12605
0.5724	1878	0.3851	-44092	0.3977	-13870
0.5921	4937	0.4097	-39036	0.4217	-14874
0.6221	4361	0.4334	-40364	0.4450	-15900
0.6262	2304	0.4558	-43695	0.4666	-16982
0.6412	14862	0.4768	-24195	0.4870	-17258
0.6431	17600	0.4965	-20005	0.5060	-17360
0.6751	21052	0.5153	-16189	0.5245	-17316
0.6813	20976	0.5331	-16585	0.5418	-17290
0.6879	21015	0.5499	-16825	0.5580	-17273
0.7224	-16689	0.5660	-16689	0.5739	-17252
<b>Section C; starting amount : n(Bi) = 5.0393mmol ; n(Sn) = 2.6557mmol</b>					
				0	94.56
0.4387	10049	0.0270	-22627	0.0539	-1131
0.4973	9570	0.0812	-26291	0.1084	-2581
0.5076	7068	0.1332	-31612	0.1580	-4193
0.5265	5409	0.1809	-35262	0.2038	-5886
0.5405	6304	0.2249	-33872	0.2460	-7368
0.5578	8020	0.2655	-31157	0.2851	-8601
0.5623	3769	0.3028	-38832	0.3206	-10102
0.5863	-4741	0.3373	-53622	0.3540	-12244
0.5978	10146	0.3694	-28563	0.3849	-13023
0.5981	13679	0.3989	-22666	0.4130	-13463
0.5997	7688	0.4258	-32714	0.4386	-14306
0.6080	22174	0.4506	-9065	0.4625	-14083
0.6082	19340	0.4734	-13737	0.4844	-14069
0.6094	18897	0.4945	-14525	0.5046	-14087
0.6116	18899	0.5140	-14634	0.5234	-14108
0.6228	19966	0.5322	-13476	0.5411	-14084
0.6255	19822	0.5493	-13844	0.5576	-14076
0.6346	19774	0.5654	-14377	0.5732	-14086
0.6407	20243	0.5805	-13940	0.5878	-14081
0.6595	20687	0.5948	-14166	0.6019	-14084
0.6624	20909	0.6085	-13968	0.6151	-14080
0.6636	20890	0.6212	-14056	0.6274	-14079

Mole dropped $n_{Ni}$ (mmol)	Heateffect $Q(J)$	Partial enthalpy		Integralenthalpy	
		$x_{Ni}^*$	$\overline{\Delta H}_{Ni}(J.mol^{-1})$	$x_{Ni}$	$\Delta_{mix}H(J.mol^{-1})$
0.6646	20594	0.6332	-14549	0.6390	-14094
0.6774	21058	0.6446	-14449	0.6502	-14105
<b>Section D; starting amount : n(Bi) = 5.3367mmol ; n(Sn) = 1.8679mmol</b>					
				0	80.27
0.4573	11714	0.0298	-19920	0.0597	-1113
0.4656	9579	0.0866	-24963	0.1136	-2480
0.4817	5085	0.1384	-34979	0.1632	-4298
0.4879	5520	0.1856	-34222	0.2080	-5903
0.4888	4540	0.2282	-36247	0.2484	-7451
0.5171	-5786	0.2677	-56726	0.2869	-9973
0.5239	-442	0.3045	-46379	0.3221	-11767
0.5359	8589	0.3383	-29506	0.3546	-12619
0.5359	12978	0.3694	-21316	0.3842	-13017
0.5387	20534	0.3977	-7416	0.4113	-12771
0.5413	16140	0.4237	-15719	0.4362	-12896
0.5427	16596	0.4477	-14954	0.4592	-12979
0.5429	17296	0.4698	-13676	0.4804	-13007
0.5431	17283	0.4901	-13712	0.4999	-13033
0.5460	20306	0.5091	-8343	0.5182	-12862
0.5552	18355	0.5268	-12475	0.5354	-12848
0.5555	17064	0.5435	-14818	0.5515	-12916
0.5556	18006	0.5590	-13126	0.5665	-12923
0.5562	17308	0.5735	-14414	0.5805	-12972
0.5680	17633	0.5873	-14491	0.5940	-13020
0.5933	18138	0.6005	-14962	0.6071	-13083
0.6001	18500	0.6133	-14707	0.6196	-13135
0.6139	18896	0.6255	-14753	0.6315	-13185
0.6288	19371	0.6372	-14731	0.6430	-13233
0.6540	20212	0.6486	-14628	0.6542	-13277
<b>Section E; starting amount : n(Bi) = 6.2364 mol ; n(Sn) = 0.7652 mmol</b>					
				0	39.81
0.3630	6275	0.0635	-24767	0.0430	-578
0.4019	2012	0.1029	-33542	0.0840	-1615
0.4086	2351	0.1394	-45282	0.1219	-2934
0.4247	9834	0.1732	-36618	0.1569	-4624
0.4394	15021	0.2047	-31599	0.1894	-5859
0.4501	18241	0.2342	-18697	0.2200	-6828
0.4555	13331	0.2618	-10028	0.2484	-7261
0.9369	32091	0.3263	-13122	0.2752	-7360
0.5236	22034	0.4260	-15527	0.3566	-7754
0.5310	22177	0.4506	-16177	0.3861	-7641
0.5345	17022	0.4736	-15926	0.4134	-7550
0.5574	17388	0.4950	-16007	0.4386	-7892
0.5579	17544	0.5149	-16028	0.4626	-8247
0.5661	17758	0.5335	-16571	0.4846	-8562
0.5744	18007	0.5509	-17298	0.5053	-8860
0.5771	17775	0.5671	-17227	0.5246	-9139
0.5837	17554	0.5823	-16147	0.5593	-9709
0.5864	17679	0.5965	-15771	0.5750	-9977
0.5866	18318	0.6098	-15827	0.6033	-10376
0.5904	18660	0.6224	-16856	0.6163	-10554
0.5960	18801	0.6344	-16615	0.6403	-10941
0.5979	18248	0.6464	-15724	0.6524	-11101
<b>Section F; starting amount : n(Bi) = 4.5965mmol ; n(Ni) = 1.1591mmol</b>					
				0	-1149
0.3484	-7961	0.0285	-57832	0.0571	-4384
0.3957	-13390	0.0858	-68816	0.114	-8306
				5	
0.4024	4451	0.1403	-23915	0.166	-9216
				1	
0.4065	12981	0.1893	-3043	0.2125	-8873
0.4073	15901	0.2333	4060	0.2541	-8190
0.4130	17498	0.2730	7392	0.2919	-7399
0.4162	19044	0.3092	10782	0.3264	-6513

Mole dropped $n_{Ni}$ (mmol)	Heateffect $Q(J)$	Partial enthalpy		Integralenthalpy	
		$x_{Ni}^*$	$\overline{\Delta H}_{Ni}(J.mol^{-1})$	$x_{Ni}$	$\Delta_{mix}H(J.mol^{-1})$
0.4467	20824	0.3432	11642	0.3599	-5611
0.4539	22013	0.3753	13517	0.3907	-4692
0.4592	21874	0.4048	12655	0.4189	-3888
0.4669	15190	0.4320	-2444	0.4451	-3823
0.4670	15256	0.4570	-2308	0.4690	-3757
0.4728	15480	0.4801	-2236	0.4912	-3694
0.4757	15743	0.5014	-1886	0.5117	-3621
0.4898	16204	0.5214	-1896	0.5312	-3552
0.4915	16355	0.5402	-1702	0.5492	-3481
0.4961	16450	0.5577	-1821	0.5661	-3419
0.4976	16576	0.5739	-1670	0.5818	-3356
0.5024	16275	0.5891	-2581	0.5965	-3328
0.5163	17415	0.6036	-1250	0.6106	-3256
0.5232	17783	0.6173	-987	0.623	-3178
0.5249	17598	0.6302	-1449	0.6364	-3121
0.5289	14573	0.6423	-7425	0.6481	-3260
0.5391	17770	0.6538	-2015	0.6594	-3220
0.5420	18276	0.6647	-1255	0.6700	-3159
<b>Section G; starting amount : n(Bi) 3.3582mmol ; n(Ni) = 1.0769mmol</b>					
				0	-1268
0.1931	-3912	0.0209	-55234	0.0417	-3520
0.2195	-14799	0.0634	-102399	0.0851	-7997
0.2330	-8258	0.1061	-70419	0.1271	-10860
0.2452	794	0.1472	-31741	0.1673	-11821
0.2490	6105	0.1859	-10464	0.2045	-11761
0.2618	9717	0.2223	2134	0.2401	-11137
0.2686	10940	0.2569	5743	0.2736	-10395
0.2737	11757	0.2892	7972	0.3048	-9607
0.2755	12455	0.3191	10231	0.3335	-8785
0.2843	13608	0.3472	12893	0.3608	-7897
0.2849	13348	0.3734	11877	0.3860	-7117
0.2853	14345	0.3977	15297	0.4094	-6266
0.2957	14476	0.4206	13977	0.4317	-5499
0.3080	14617	0.4425	12483	0.4533	-4816
0.3089	10014	0.4633	-2563	0.4734	-4734
0.3197	10336	0.4830	-2648	0.4926	-4657
0.3398	10964	0.5021	-2710	0.5116	-4584
0.3410	11280	0.5205	-1896	0.5293	-4487
0.3428	11141	0.5376	-2481	0.5458	-4417
0.3644	12131	0.5540	-1690	0.5622	-4319
0.3678	12329	0.5698	-1459	0.5775	-4218
0.3716	12232	0.5847	-2061	0.5919	-4145
0.3741	12392	0.5987	-1850	0.6055	-4068
0.3782	12813	0.6119	-1099	0.6184	-3972
0.3788	12671	0.6244	-1526	0.6304	-3894
<b>Section H; starting amount : n(Bi) = 3.8149mmol ; n(Ni) = 1.6367mmol</b>					
				0	-1365
0.3025	-11616	0.0263	-73375	0.0526	-5151
0.3317	-22107	0.0784	-101632	0.1042	-10409
0.3444	-15165	0.1282	-79010	0.1522	-14083
0.3476	634	0.1739	-48660	0.1957	-15770
0.3585	9561	0.2159	-14152	0.2361	-15690
0.3621	13450	0.2545	2168	0.2730	-13906
0.3709	15824	0.2901	7691	0.3072	-12889
0.4025	18406	0.3241	10748	0.3409	-11738
0.4120	19439	0.3566	12207	0.3722	-10602
0.4200	20829	0.3867	14619	0.4012	-9439
0.4295	21511	0.4147	15108	0.4281	-8333
0.4393	22953	0.4407	17276	0.4533	-7205
0.4455	22829	0.4650	16266	0.4767	-6201
0.4629	21266	0.4878	10959	0.4990	-5471
0.4694	15048	0.5093	-2922	0.5197	-5366
0.4864	15851	0.5296	-2387	0.5394	-5243

Mole dropped $n_{Ni}$ (mmol)	Heateffect $Q(J)$	Partial enthalpy		Integralenthalpy	
		$x_{Ni}^*$	$\overline{\Delta H_{Ni}}(J.mol^{-1})$	$x_{Ni}$	$\Delta_{mix}H(J.mol^{-1})$
0.4940	16105	0.5487	-2379	0.5579	-5129
0.4949	16256	0.5664	-2129	0.5749	-5013
0.5051	16554	0.5830	-2202	0.5910	-4906
0.5120	16823	0.5986	-2123	0.6062	-4803
0.5174	17157	0.6133	-1815	0.6204	-4696
0.5347	17730	0.6272	-1820	0.6340	-4593
0.5347	17922	0.6403	-1461	0.6467	-4484
0.5388	18042	0.6526	-1496	0.6586	-4383
0.5405	18100	0.6642	-1492	0.6698	-4288

$x^*$  Average value before and after each drop.

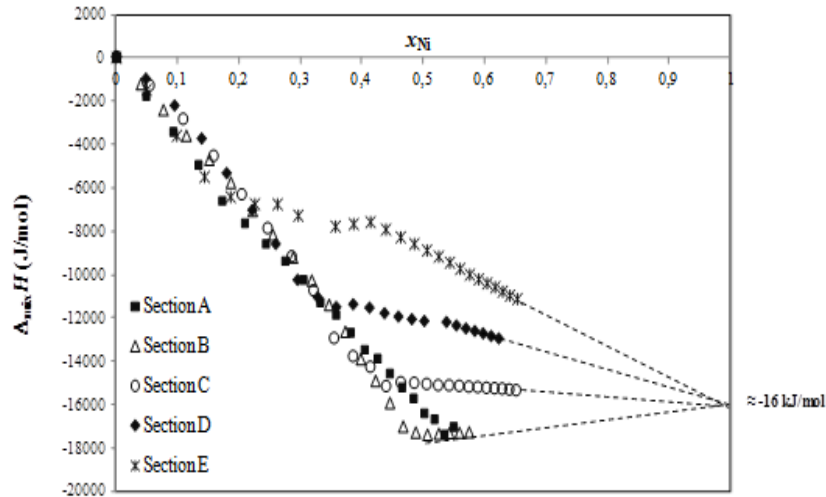


**Figure 2.** Integral molar enthalpies of mixing at 1000°C in the Bi-Ni-Sn liquid alloys along sections investigated by dropping nickel to  $Bi_xSn_{1-x}$ . (Standard states: pure liquid metals).

**Table 3.** The coordinate values of kink according to investigated section.

Section	B	C	D	E
$x_{Ni}(Kink)$	0,47	0,43	0,38	0,25
$\Delta_{mix}H(Kink)$	-17000	-14300	-13000	-6730

The curves representing the partial enthalpies show complex shapes, and to obtain a more visible and clear graph, we give here only the example of three isopleths (Figure 3). The kink observed in  $\Delta_{mix}H = f(x_{Ni})$  curves (Figure 2) are in agreement with the jump of  $\overline{\Delta H_M}$  values at the same composition of nickel. This trend could be due to the appearance of the solid phase of nickel. From this biphasic domain (solid-liquid), the partial values remain almost constant with a value close to -16 kJ/mol (Figures 2 and 3), which would correspond to that of the enthalpy of fusion of pure Ni. While the absence of the kink in section A clearly shows that  $(Bi_{0,34}Sn_{0,66})_{1-x}Ni_x$  alloys are in the liquid state along with the whole experimental range of composition at 1000°C.

On the other hand, for sections (F, G, and H) investigated by dropping tin to  $Bi_xNi_{1-x}$  alloys, the integral enthalpy decreases highly from the first drops of tin to reach a minimum increase rapidly (Figure 4). From an approximate composition of 40-50 at. % of tin (depending on the studied section), the integral enthalpy increases linearly and moderately to reach zero value corresponding to the enthalpy of formation of pure tin. The minimum observed in the integral enthalpies reaches the values of about -9000 (section F), -12000 (section G), and -15000 J/mol (section H). This shows that as the alloys become richer in nickel, the interactions between the metals increase, and thus the enthalpies become more negative (exothermic).



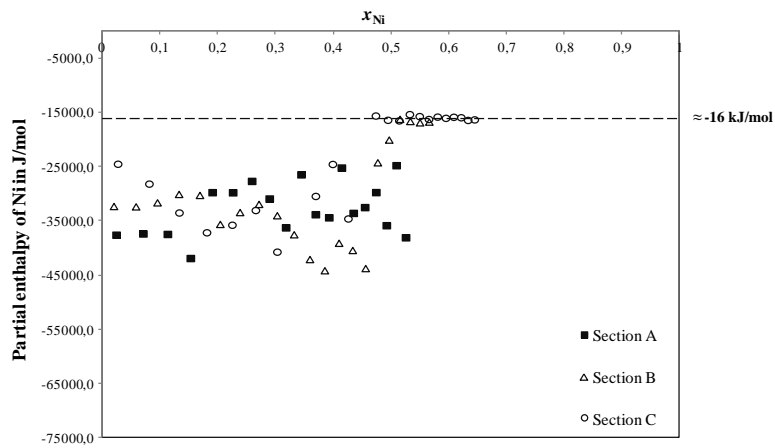


**Figure 3.** Partial molar enthalpies of Ni in the Bi-Ni-Sn liquid alloys at 1000°C along sections investigated by dropping nickel to  $\text{Bi}_x\text{Ni}_{1-x}$ . (Standard states: pure liquid metals).

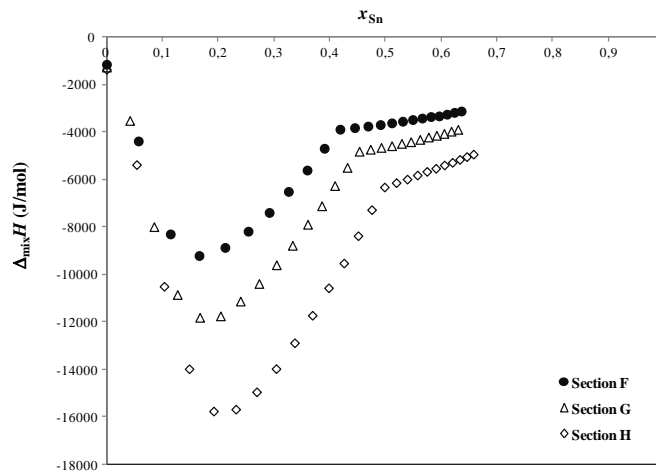


**Figure 4.** Integral molar enthalpies of mixing in the Bi-Ni-Sn liquid alloys at 1000°C along sections investigated by dropping tin to  $\text{Bi}_x\text{Ni}_{1-x}$ . (Standard states: pure liquid metals).

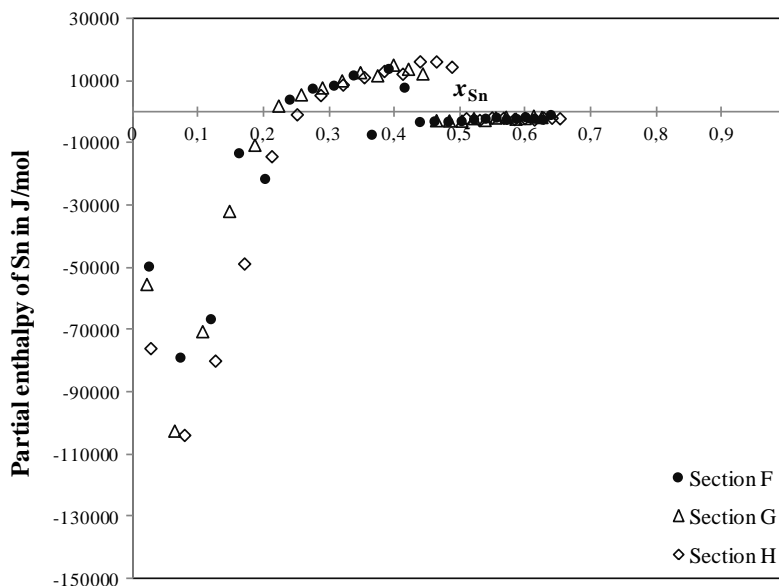


**Figure 5.** Partial molar enthalpies of Sn in the Bi-Ni-Sn liquid alloys at 1000°C along sections investigated by dropping tin to  $\text{Bi}_x\text{Ni}_{1-x}$ . (Standard states: pure liquid metals).

Furthermore, the partial enthalpy curves as a function of tin addition show three distinct parts: the values start to be exothermic in the range composition 0-22 at.% Sn, then become

endothermic between 22 and 45 at.% Sn to finally take the value zero (Figure 5), indicating an almost ideal mixing behavior for additions of Sn to the binary Bi–Ni alloys.

The points of intersection between the different sections make it possible to check the coherence of our calorimetric results.

In fact, two ternary alloys of the same composition obtained either by adding nickel to a liquid Bi-Sn binary alloy or by adding tin to a liquid Ni-Sn binary alloy must have the same values of the enthalpy of mixing. The points of intersection between sections A-E and F-H are illustrated in Figure 6.

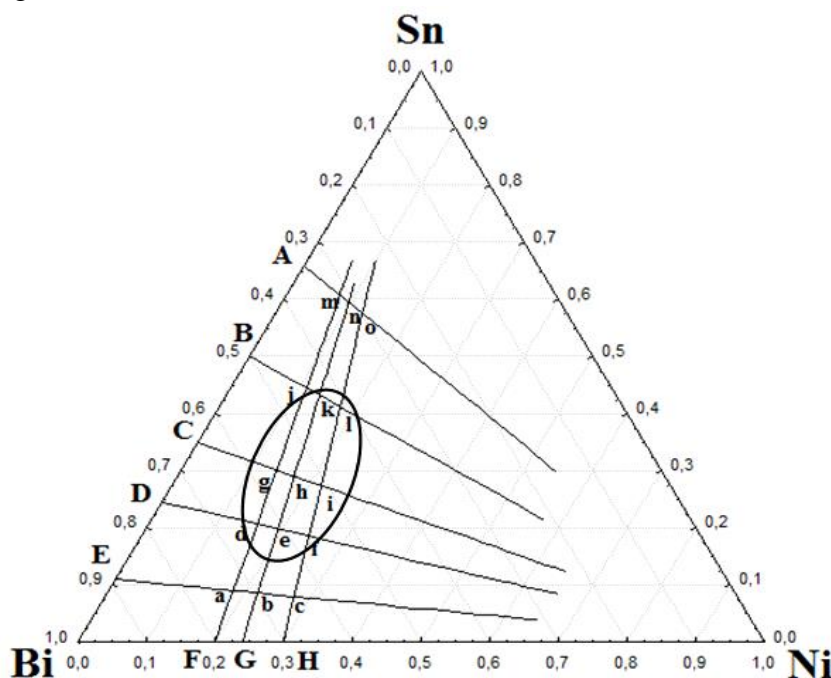


**Figure 6.** Points of intersection (a-o) between investigated sections. The points where the difference is significant (d-i, k, and l) are inside the area indicated in the triangle.

The differences observed between  $\Delta_{\text{mix}}H$  values at the intersection point a-c, j and m-o remain acceptable and do not exceed 433J/mol (Table 4). However, for other points of intersection, the difference between the measured values is important and can reach the value of 7500J/mol (Table 4).

**Table 4.** Values of the enthalpy of mixing at the interaction points (a-o) (see Figure 6).

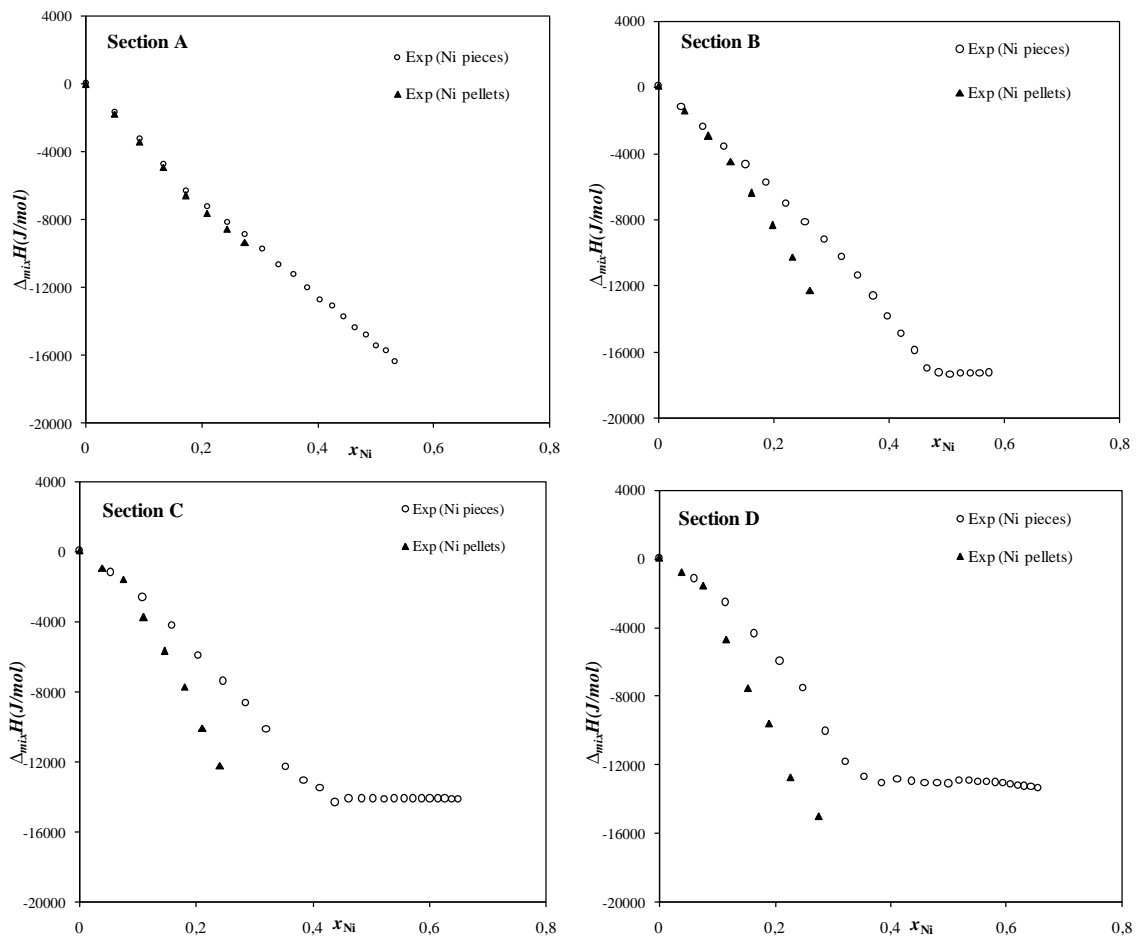
Intersection points	Mole fraction		$\Delta_{\text{mix}}H(\text{J/mol})$		Difference (J/mol)
	$x_{\text{Ni}}$	$x_{\text{Sn}}$	Ni (pieces)	Sn	
a(E.F)	0.185	0.082	-6334	-6149	185
b(E.G)	0.230	0.080	-6825	-7258	433
c(E.H)	0.270	0.073	-6921	-7056	135
d(D.F)	0.160	0.210	-4217	-8929	4712
e(D.G)	0.200	0.200	-5644	-11746	6102
f(D.H)	0.240	0.190	-7321	-14864	7543
g(C.F)	0.140	0.300	-3961	-7289	3328
h(C.G)	0.180	0.285	-5472	-10159	4687
i(C.H)	0.220	0.270	-6851	-13842	6991
j(B.F)	0.112	0.445	-3659	-3850	191
k(B.G)	0.142	0.425	-4489	-5780	1291
l(B.H)	0.180	0.410	-5526	-8953	3427
m(A.F)	0.080	0.610	-2843	-3268	425
n(A.G)	0.105	0.590	-4010	-4193	183
o(A.H)	0.130	0.572	-4740	-5013	273

The concerned area (d-i, k, and l) is delimited in the Gibbs triangle, as shown in Figure 6. To explain these differences, we supposed firstly that this phenomenon could be due to a problem of dissolution of the nickel, which has a very high melting point (1455°C). In order to overcome this problem, we measured the same sections (A-E) for a second time by adding Ni pellets instead of pieces. The results obtained are collected in Table 5.

**Table 5.** Integral enthalpies of mixing in the liquid Bi-Ni-Sn alloys by adding Ni pellets to Bi<sub>x</sub>Sn<sub>1-x</sub> alloys at 1000°C.

Section A		Section B		Section C		Section D		Section E	
$x_{Ni}$	$\Delta_{mix}H$ (J.mol <sup>-1</sup> )	$x_{Ni}$	$\Delta_{mix}H$ (J.mol <sup>-1</sup> )	$x_{Ni}$	$\Delta_{mix}H$ (J.mol <sup>-1</sup> )	$x_{Ni}$	$\Delta_{mix}H$ (J.mol <sup>-1</sup> )	$x_{Ni}$	$\Delta_{mix}H$ (J.mol <sup>-1</sup> )
0	94.07	0	105	0	94.56	0	80.27	0	39.81
0.0471	-1735	0.0447	-1400	0.0392	-871	0.0388	-760	0.0493	-1444
0.0912	-3389	0.0865	-2934	0.0755	-1555	0.0760	-1547	0.0985	-3562
0.1342	-4915	0.1253	-4500	0.1100	-3724	0.1157	-4691	0.1435	-5464
0.1728	-6567	0.1611	-6384	0.1461	-5638	0.1532	-7532	0.1858	-6391
0.2099	-7597	0.1979	-8341	0.1800	-7702	0.1896	-9596	0.2254	-6721
0.2430	-8553	0.2317	-10265	0.2114	-10025	0.2266	-12737	0.2622	-6727
0.2751	-9348	0.2630	-12254	0.2413	-12201	0.2753	-15008	0.2960	-7248

For comparison, Figure 7 shows the results obtained by adding Ni pellets and those obtained by adding Ni pieces.



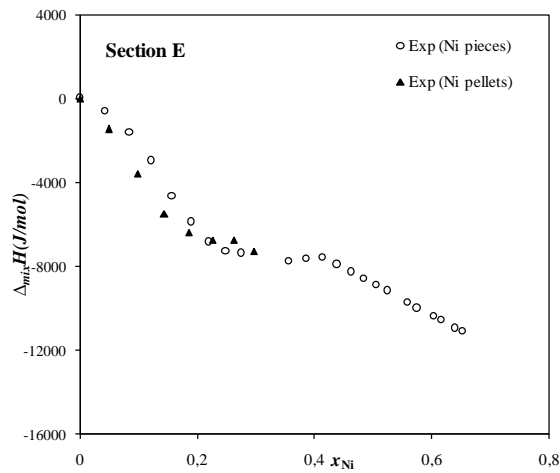


**Figure 7.** Integral molar enthalpies of mixing at 1000°C in liquid Bi-Ni-Sn alloys by adding Ni (pieces and pellets) to the  $\text{Bi}_x\text{Ni}_{1-x}$  alloys. Standard states: pure liquid metals.

As it can be seen from Figure 7 and Table 5, the results obtained for both the Ni pieces and the Ni pellets are very similar for sections A and E, which are situated outside the area delimited in the Gibbs triangle (Figure 6). The results for sections B, C, and D show that the enthalpies obtained by adding nickel pellets are more exothermic than those obtained by adding Ni pieces. More probably, the fact that using the nickel pellets has increased its dissolution within the mixture, and thus the enthalpy of mixing becomes more negative. The results obtained for the nickel in pellet led to a clear improvement of the enthalpies at the intersection points. However, as can be seen from Table 6, some differences still appear significant. This difference could probably be explained by the possibility of a miscibility gap in the Bi-Ni-Sn liquid phase (See the area delimited in the triangle of Figure 6). It is important to note that this behavior has been reported in the Bi-Ni binary system by Vassilev *et al.* [23] and in Bi-Ni-Sn ternary system by Milcheva *et al.* [42], studying activity coefficients and using the isopiestic method.

**Table 6.** Values of the enthalpy of mixing at the intersection points (a-o) obtained by nickel pellets addition and by tin addition.

Intersection points	$\Delta_{mix}H$ (J/mol)			Difference (J/mol) (Ni pellets Addition)	Difference (J/mol) (Ni pieces Addition)
	Ni pellets addition	*Ni pieces addition	Sn addition		
a(E.F)	-5708	-6334	-6149	441	185
b(E.G)	-7051	-6825	-7258	207	433
c(E.H)	-7303	-6921	-7056	247	135
d(D.F)	-7991	-4217	-8929	938	4712
e(D.G)	-10754	-5644	-11746	992	6102
f(D.H)	-13389	-7321	-14864	1475	7543
g(C.F)	-5406	-3961	-7289	1883	3328
h(C.G)	-7774	-5472	-10159	2385	4687
i(C.H)	-10594	-6851	-13842	3248	6991
j(B.F)	-4035	-3659	-3850	185	191
k(B.G)	-5550	-4489	-5780	230	1291
l(B.H)	-7389	-5526	-8953	1564	3427
m(A.F)	-2966	-2843	-3268	302	425
n(A.G)	-3730	-4010	-4193	463	183
o(A.H)	-4791	-4740	-5013	222	273

\* The values of nickel pieces are added in table for comparison.

The experimental results for ternary Bi-Ni-Sn alloys have been represented by the Redlich-Kister-Muggianu polynomial [43].

The experimental ternary interaction parameters are presented in Table 7.

**Table 7.** Binary and ternary interaction parameters in the liquid Bi-Ni-Sn system.

Interaction parameter	T (°C)	$v, \alpha$	J/mol	Reference
$L_{Bi-Sn}^{(v)}$	400	0	442	[33]
		1	-298	
$L_{Bi-Ni}^{(v)}$	1000-1300	1	-4792	[26]
		2	-5916	
		3	3135	
$L_{Ni-Sn}^{(v)}$	1000	0	-76856	[36]
		1	-36997	
$M_{Bi-Ni-Sn}^{(\alpha)}$	1000	0	-454367	This work
		1	-556282	
		2	324872	

Figures 8 and 9 show an iso-enthalpy plot and tridimensional surface of integral enthalpy values for ternary Bi-Ni-Sn liquid alloys. The values are generally negative, with a minimum of about -20 kJ/mol.

The second part of this work concerns the estimation of the integral enthalpy of mixing using geometrical models.

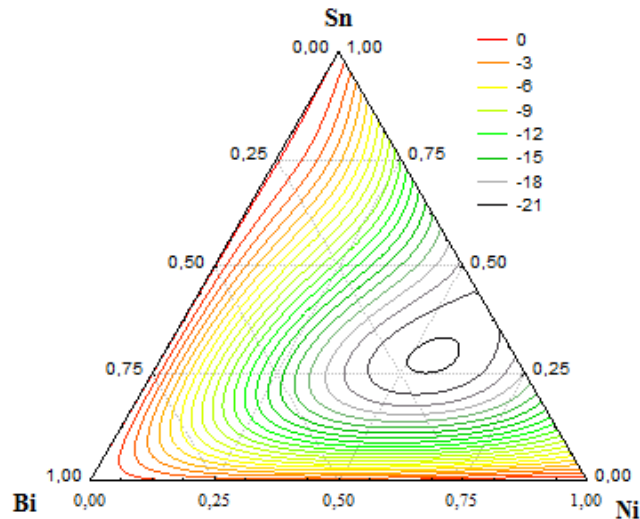


**Figure 8.** Iso-enthalpy curves (kJ/mol) of the ternary Bi-Ni-Sn system at 1000°C, standard states: pure liquid metals.

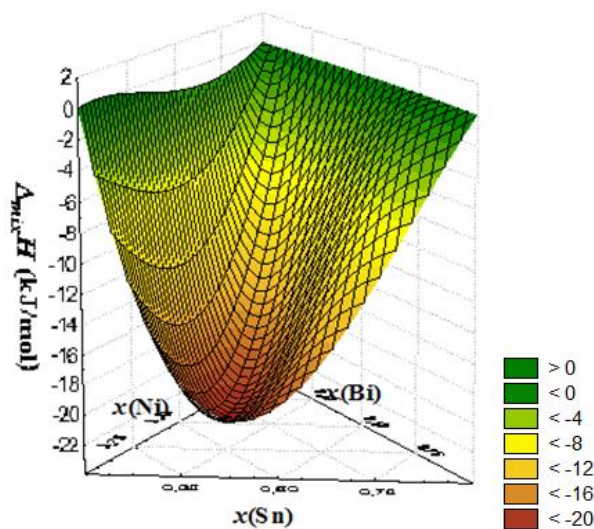


**Figure 9.** 3D surface representation of the enthalpy of mixing of liquid Bi-Ni-Sn alloys at 1000°C; standard state: pure liquid components.

5.2. Extrapolated models.

Figure 10 shows the calculated enthalpy versus nickel composition for sections A-E using the models of Kohler, Toop, and Chou and the experimental values for comparison.

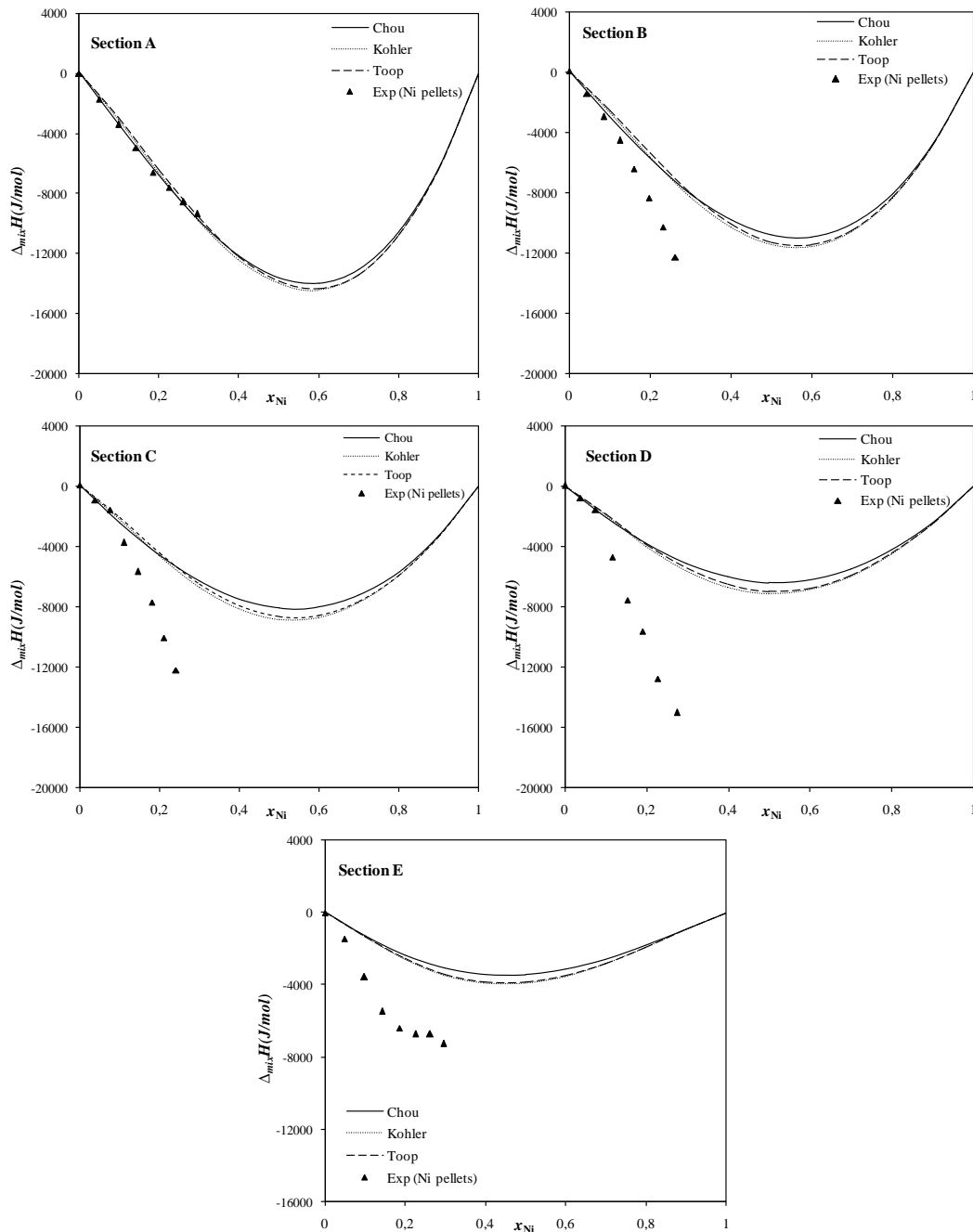


**Figure 10.** Experimental and calculated integral enthalpy of mixing  $\Delta_{mix}H = f(x_{Ni})$  in liquid Bi-Ni-Sn at 1000°C.

The analysis of the results shows that the experimental values are more exothermic than estimated ones, with the exception of the Sn-rich section (A), where the two results are very similar. In addition, it is important to note that the more the section is rich in bismuth more important the difference between the experimental and calculated results (from section B to section D). In the case of section E, the difference is less significant compared to sections B-D. Moreover, as we have already suggested, sections A and E alloys are located outside the area delimited in Figure 6 of the Gibbs triangle (zone assumed to contain an immiscible liquid phase).

Figure 11 represents the calculated mixing enthalpy as a function of tin compositions along sections F-H and using the same theoretical models. It can be seen that for alloys containing more than 45 at.% Sn, the experimental and estimated results are in good agreement. This composition domain is located outside the zone indicated in the triangle of Figure 6. Nevertheless, for alloys with less than 45 at. % Sn, the difference becomes very important. Indeed, in this range of compositions (0-45 at.% Sn), the presence of the "well of enthalpy" in experimental values could probably confirm a possible existence of a miscibility gap. The measured enthalpies, in this case, are very different from those calculated.

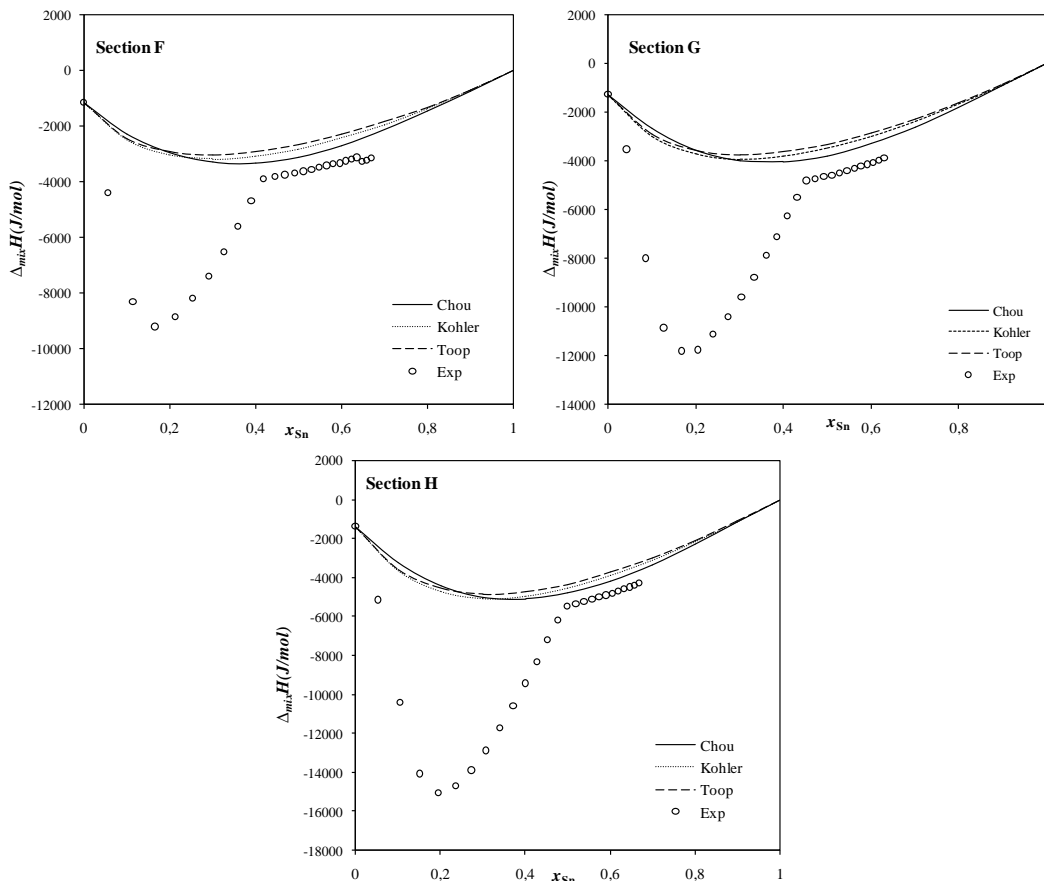


**Figure 11.** Experimental and calculated integral enthalpy of mixing  $\Delta_{mix}H = f(x_{Sn})$  in liquid Bi-Ni-Sn at 1000°C.

## 6. Conclusions

In the present paper, the partial and integral enthalpies of liquid ternary Bi-Ni-Sn alloys were measured at 1000°C by adding nickel to  $Bi_xSn_{1-x}$  and tin to  $Bi_xNi_{1-x}$ . Indeed, the integral enthalpy of mixing has been estimated using Kohler as a symmetric model, Toop as an asymmetric model, and Chou as a general solution model. All measured and calculated values are exothermic over the explored domain. However, a difference between the measured and estimated values has been reported. This difference becomes very remarkable in a limited region of the Gibbs triangle. As has already been reported in certain previous works, this region could probably correspond to a zone of liquid immiscibility. Further work remains essential to confirm this conclusion.

## Funding

This research received no external funding.

## Acknowledgments

Two authors (Pr. A. Sabbar and Dr. M. Rechchach) wish to thank the "Department of Inorganic Chemistry - Functional Materials" team at Vienna University, particularly Professor Hans Flandorfer, who allowed us to carry out the calorimetric measurements.

## Conflicts of Interest

The authors declare no conflict of interest.

## References

1. Directive 2002/95/EC. Directive 2002/95/EC of the European Parliament and of the Council of 27 January 2003 on the restriction of the use of certain hazardous substances in electrical and electronic equipment. *Official Journal of the European Union L37* **2003**, *17*, 19–23, <http://data.europa.eu/eli/dir/2002/95/oj>.
2. Rashidi, R.; Naffakh-Moosavy, H. Metallurgical, physical, mechanical and oxidation behavior of lead-free chromium dissolved Sn–Cu–Bi solders. *Journal of Materials Research and Technology* **2021**, *13*, 1805–1825, <https://doi.org/10.1016/j.jmrt.2021.05.055>.
3. Rashidi, R.; Naffakh-Moosavy, H. The influence of chromium addition on the metallurgical, mechanical and fracture aspects of Sn–Cu–Bi/Cu solder joint. *Journal of Materials Research and Technology* **2021**, *15*, 3321–3336, <https://doi.org/10.1016/j.jmrt.2021.10.015>.
4. Pal, M.K.; Gergely, G.; Koncz-Horváth, D.; Gácsi, Z. Investigation of microstructure and wetting behavior of Sn–3.0Ag–0.5Cu (SAC305) lead-free solder with additions of 1.0 wt % SiC on copper substrate. *Intermetallics* **2021**, *128*, 106991, <https://doi.org/10.1016/j.intermet.2020.106991>.
5. Hassan, K.M.R.; Wu, J.; Alam, M.S.; Suhling, J.C.; Lall, P. Mechanical Behavior and Reliability of SAC+Bi Lead Free Solders with Various Levels of Bismuth. 2021 IEEE 71st Electronic Components and Technology Conference (ECTC), San Diego, CA, USA, 1 June–4 July 2021, IEEE, **2021**, <https://doi.org/10.1109/ECTC32696.2021.00155>.
6. Hoque, M.A.; Haq, M.A.; Suhling, J.C.; Lall, P. Mechanical Behavior and Microstructure Evolution in Lead Free Solders Subjected to Mechanical Cycling at Elevated Temperatures. 2021 IEEE 71st Electronic Components and Technology Conference (ECTC), San Diego, CA, USA, 1 June–4 July 2021, IEEE, **2021**, <https://doi.org/10.1109/ECTC32696.2021.00366>.
7. Hoque, M.A.; Haq, M.A.; Suhling, J.C.; Lall, P. Effect of Bismuth Content on the Mechanical Cyclic Properties of SAC+Bi Lead Free Solders. 2021 IEEE 71st Electronic Components and Technology Conference (ECTC), San Diego, CA, USA, 1 June–4 July 2021, IEEE, **2021**, <https://doi.org/10.1109/ECTC32696.2021.00284>.
8. Sonawane, P.D.; Bupesh Raja, V.K.; Gupta, M. Mechanical properties and corrosion analysis of lead-free Sn-0.7Cu solder CSI joints on Cu substrate. *Materials Today: Proceedings* **2021**, *46*, 1101–1105, <https://doi.org/10.1016/j.matpr.2021.01.521>.
9. Li, Q.; Zhao, M.; Lin, J.; Lu, S. Effect of temperature on the corrosion behavior of lead-free solders under polyvinyl chloride fire smoke atmosphere. *Journal of Materials Research and Technology* **2021**, *15*, 3088–3098, <https://doi.org/10.1016/j.jmrt.2021.09.104>.
10. Lau, J.H. State of the Art of Lead-Free Solder Joint Reliability. *Journal of Electronic Packaging, Transactions of the ASME* **2021**, *143*, 1–36, <https://doi.org/10.1115/1.4048037>.
11. Chen, T.F.; Siow, K.S. Comparing the mechanical and thermal-electrical properties of sintered copper (Cu) and sintered silver (Ag) joints. *Journal of Alloys and Compounds* **2021**, *866*, 158783, <https://doi.org/10.1016/j.jallcom.2021.158783>.
12. Ali, U.; Khan, H.; Aamir, M.; Giasin, K.; Habib, N.; Owais Awan, M. Analysis of microstructure and mechanical properties of bismuth-doped SAC305 lead-free solder alloy at high temperature. *Metals* **2021**, *11*, 1077, <https://doi.org/10.3390/met11071077>.
13. Faizan, M. Lead-Free Solders: Overview, Challenges, and Solutions. In *Advances in Interdisciplinary Engineering*, **2021**, 321–325, [https://doi.org/10.1007/978-981-15-9956-9\\_32](https://doi.org/10.1007/978-981-15-9956-9_32).
14. Yang, W.; Mao, J.; Ma, Y.; Yu, S.; He, H.; Qi, D.; Zhan, Y. Effects of yttrium addition on the microstructure evolution and electrochemical corrosion of Sn-9Zn lead-free solders alloy. *Materials* **2021**, *14*, 2549, <https://doi.org/10.3390/ma14102549>.



15. Steiner, F.; Hirman, M.; Prosr, P.; Rous, P. Properties Verification of Improved Lead-free Solder Alloys. , *2021 44th International Spring Seminar on Electronics Technology (ISSE)*, **2021**, 1–5, <https://doi.org/10.1109/ISSE51996.2021.9467573>.
16. Mazullah; Sadiq, M.; Khan, M.; Mateen, A.; Shahzad, M.; Akhtar, K.; Khan, J. Thermal aging impact on microstructure, creep and corrosion behavior of lead-free solder alloy (SAC387) use in electronics. *Microelectronics Reliability* **2021**, *122*, 114180, <https://doi.org/10.1016/j.microrel.2021.114180>.
17. Vassilev, G.P.; Lilova, K.I.; Gachon, J.C. Calorimetric and phase equilibria studies of the Ni-Sn-Bi system. *Crystal Research and Technology* **2008**, *43*, 980–985, <https://doi.org/10.1002/crat.200800121>.
18. Kohler, F. Zur Berechnung der thermodynamischen Daten eines ternären Systems aus den zugehörigen binären Systemen - Kurze Mitteilung. *Monatshefte für Chemie* **1960**, *91*, 738–740, <https://doi.org/10.1007/BF00899814>.
19. TOOP, G.W. Predicting ternary activities using binary data. *Trans Metall Soc AIME* **1965** , *233*, 850–855.
20. Chou, K.C. A general solution model for predicting ternary thermodynamic properties. *Calphad* **1995**, *19*, 315–325, [https://doi.org/10.1016/0364-5916\(95\)00029-E](https://doi.org/10.1016/0364-5916(95)00029-E).
21. Predel, B.; Ruge, H. Bildungsenthalpien und bindingsverhältnisse in einigen intermetallischen verbindungen vom NiAs-Typ. *Thermochimica Acta* **1972**, *3*, 411–418, [https://doi.org/10.1016/0040-6031\(72\)87055-2](https://doi.org/10.1016/0040-6031(72)87055-2).
22. Perring, L.; Kuntz, J.J.; Bussy, F.; Gachon, J.C. Heat capacity measurements by differential scanning calorimetry in the Pd-Pb, Pd-Sn and Pd-In systems. *Thermochimica Acta* **2001**, *366*, 31–36, [https://doi.org/10.1016/S0040-6031\(00\)00731-0](https://doi.org/10.1016/S0040-6031(00)00731-0).
23. Vassilev, G.P.; Romanowska, J.; Wnuk, G. Bismuth activity measurements and thermodynamic re-optimization of the Ni-Bi System. *International Journal of Materials Research* **2007**, *98*, 468–475, <https://doi.org/10.3139/146.101499>.
24. Samui, P.; Agarwal, R.; Padhi, A.; Kulkarni, S.G. Thermodynamic investigations of Bi-Ni system - Part I. *Journal of Chemical Thermodynamics* **2013**, *57*, 470–476, <https://doi.org/10.1016/j.jct.2012.09.024>.
25. Agarwal, R.; Samui, P.; Kulkarni, S.G. Thermodynamic investigations of (Bi + Ni) system - Part II. *Journal of Chemical Thermodynamics* **2013**, *57*, 477–484, <https://doi.org/10.1016/j.jct.2012.09.010>.
26. El Maniani, M.; Rechchach, M.; El Mahfoudi, A.; El Moudane, M.; Sabbar, A. A Calorimetric investigation of the liquid bi-ni alloys. *Journal of Materials and Environmental Science* **2016**, *7*, 3759–3766.
27. Fima, P.; Flandorfer, H. Mixing enthalpies of liquid Bi–Ni and Ag–Bi–Ni alloys. *Thermochimica Acta* **2017**, *657*, 134–143, <https://doi.org/10.1016/j.tca.2017.09.002>.
28. Hultgren, R.; Desai, P.D.; Hawkins, D.T.; Gleiser, M.; Kelley, K.K. Selected values of the thermodynamic properties of binary alloys. *National Standard Reference Data System* **1973**.
29. Yazawa, A.; Kawashima, T.; Itagaki, K. Measurements of Heats of Mixing in Liquid Alloys with the Adiabatic Calorimeter. *Journal of the Japan Institute of Metals* **1968**, *32*, 1281–1287, [https://doi.org/10.2320/jinstmet1952.32.12\\_1281](https://doi.org/10.2320/jinstmet1952.32.12_1281).
30. Sharkey, R.L.; Pool, M.J. Partial Heats of Mixing in the Bi-Sn system. *Metallurgical Transactions B* **1972**, *3*, 1773–1776, <https://doi.org/10.1007/BF02642560>.
31. Seltz, H.; Dunkerley, F.J. A Thermodynamic Study of the Tin-Bismuth System. *Journal of the American Chemical Society* **1942**, *64*, 1392–1395, <https://doi.org/10.1021/ja01258a044>.
32. Cho, S.A.; Camisotti, R.; Vélez, M.H. Detailed assessment of partial thermodynamic quantities of tin in molten Bi-Sn alloys from electromotive force measurements. *Metallurgical Transactions B* **1990**, *21*, 87–96, <https://doi.org/10.1007/BF02658119>.
33. Asryan, N.; Mikula, A. Thermodynamic properties of liquid Bi-Sn alloys. *Zeitschrift fuer Metallkunde/Materials Research and Advanced Techniques* **2004**, *95*, 132–135, <https://doi.org/10.3139/146.017925>.
34. Pool, M.J.; Arpshofen, I.; Predel, B.; Schultheiß, E. Ermittlung von Mischungsenthalpien flüssiger Legierungen des Systems Cu-Ni-Sn mit einem SETARAM-Hochtemperatur- Kalorimeter. *International Journal of Materials Research* **1979**, *70*, 656–659, <https://doi.org/10.1515/ijmr-1979-701006>.
35. Luck, R.; Tomiska, J.; Predel, B. Calorimetric Determination of the Enthalpy of Mixing of Liquid Nickel-Tin Alloys as a Function of Temperature. *Z. Metallkd* **1988**, *79*, 345- 349.
36. Haddad, R.; Gaune-Escard, M.; Bros, J.P.; Ranninger-Havlicek, A.; Hayer, E.; Komarek, K.L. Thermodynamics of nickel-tin liquid alloys. *Journal of Alloys and Compounds* **1997**, *247*, 82–92, [https://doi.org/10.1016/S0925-8388\(96\)02594-7](https://doi.org/10.1016/S0925-8388(96)02594-7).

37. Flandorfer, H.; Luef, C.; Saeed, U. On the temperature dependence of the enthalpies of mixing in liquid binary (Ag, Cu, Ni)-Sn alloys. *Journal of Non-Crystalline Solids* **2008**, *354*, 2953–2972, <https://doi.org/10.1016/j.jnoncrysol.2007.12.009>.
38. Glibin, V.P.; Vorobyova, T.N.; Kuznetsov, B.V. New thermodynamic assessment of nickel-tin solid and liquid alloys. *Thermochimica Acta* **2010**, *507*, 35–44, <https://doi.org/10.1016/j.tca.2010.04.026>.
39. Ghosh, G. Thermodynamic modeling of the nickel-lead-tin system. *Metallurgical and Materials Transactions A: Physical Metallurgy and Materials Science* **1999**, *30*, 1481–1494, <https://doi.org/10.1007/s11661-999-0085-x>.
40. Miettinen, J. Thermodynamic description of the Cu-Ni-Sn system at the Cu-Ni side. *Calphad: Computer Coupling of Phase Diagrams and Thermochemistry* **2003**, *27*, 309–318, <https://doi.org/10.1016/j.calphad.2003.10.001>.
41. Liu, J.; Guo, C.; Li, C.; Du, Z. Thermodynamic re-assessment of the Ni – Sn system. *International journal of materials research* **2013**, *104*, 51-59, <https://doi.org/10.3139/146.110827>.
42. Milcheva, N.; Romanowska, J.; Vassilev, G. Sn-Ni-Bi liquid phase thermodynamic properties. *Central European Journal of Chemistry* **2011**, *9*, 149–156, <https://doi.org/10.2478/s11532-010-0128-6>.
43. Muggianu, Y.M.; Gambino, M.; Bros, J.P. Enthalpy of formation of liquid Bi-Sn-Ga alloys at 723 K, choice of an analytical expression of integral and partial excess quantities of mixing. *Journal of Chemical Physics* **1975**, *72*, 83–88.